


uPA/uPAR system activation drives a glycolytic phenotype in melanoma cells

Anna Laurenzana¹, Anastasia Chillà¹, Cristina Luciani¹, Silvia Peppicelli¹, Alessio Biagioni¹, Francesca Bianchini¹, Elena Tenedini², Eugenio Torre¹, Alessandra Mocali¹, Lido Calorini¹, Francesca Margheri¹ , Gabriella Fibbi¹ and Mario Del Rosso¹

¹ Department of Experimental and Clinical Biomedical Sciences, Section of Experimental Pathology and Oncology, University of Florence, Florence, 50134, Italy

² Center for Genome Research, Life Sciences Department, University of Modena, Modena, 41125, Italy

In this manuscript, we show the involvement of the uPA/uPAR system in the regulation of aerobic glycolysis of melanoma cells. uPAR over-expression in human melanoma cells controls an invasive and glycolytic phenotype in normoxic conditions. uPAR down-regulation by siRNA or its uncoupling from integrins, and hence from integrin-linked tyrosine kinase receptors (IL-TKRs), by an antagonist peptide induced a striking inhibition of the PI3K/AKT/mTOR/HIF1 α pathway, resulting into impairment of glucose uptake, decrease of several glycolytic enzymes and of PKM2, a checkpoint that controls metabolism of cancer cells. Further, binding of uPA to uPAR regulates expression of molecules that govern cell invasion, including extracellular matrix metallo-proteinases inducer (EMPPRIN) and enolase, a glycolytic enzyme that also serves as a plasminogen receptor, thus providing a common denominator between tumor metabolism and phenotypic invasive features. Such effects depend on the α 5 β 1-integrin-mediated uPAR connection with EGFR in melanoma cells with engagement of the PI3K-mTOR-HIF α pathway. HIF-1 α trans-activates genes whose products mediate tumor invasion and glycolysis, thus providing the common denominator between melanoma metabolism and its invasive features. These findings unveil a unrecognized interaction between the invasion-related uPAR and IL-TKRs in the control of glycolysis and disclose a new pharmacological target (i.e., uPAR/IL-TKRs axis) for the therapy of melanoma.

As opposed to normal cells, that rely on mitochondrial oxidative phosphorylation to produce ATP, cancer cells, independently of oxygen tension, use glycolysis, that is a far less efficient process in terms of energy yield, although in a plenty

of glucose supply it may satisfy both energetic and biomass formation needed for proliferating cells. This feature is known as aerobic glycolysis or “Warburg effect.”¹ The increased glucose uptake by cancer cells is the rationale underlying the 18-fluoro-2-deoxyglucose positron emission tomography (18FDG-PET) imaging for diagnosis, staging and treatment monitoring of many tumors.² In addition, a limited diffusion of oxygen and an insufficient vascular bed often produce a hypoxic tumor microenvironment³ that promotes in cancer cells a constitutive up-regulation of anaerobic glycolysis under the influence of HIF-1 α transcription factor.^{4,5} Hypoxia-stabilized HIF1 α subunit trans-activates a set of genes accounting for glycolysis activation, such as glucose transporter 1 (GLUT1), lactate dehydrogenase A (LDH-A) and other glycolytic enzymes.⁵ HIF-1 α can also be activated under normoxic conditions by oncogenic signaling pathways, including PI3K, and by mutations in tumor suppressor proteins, such as VHL (Von Hippel Lindau), succinate dehydrogenase, fumarate hydratase [reviewed in Ref. 6], indicating that in cancer cells activation of the glycolytic pathway is an effect of genome instability leading to reprogramming pyruvate oxidation to lactic acid conversion. Abnormalities of blood and lymphatic networks, high growth rate and aerobic/anaerobic glycolysis contribute to reduce pH in tumor extracellular space (primarily lactic acidosis).^{5,7} Microenvironment acidification is actually considered a new hallmark of

Key words: uPA/uPAR system, cancer cell metabolism, melanoma cells

Additional Supporting Information may be found in the online version of this article.

A. L. and A. C. contributed equally to this study.

Grant sponsor: Associazione Italiana Ricerca sul Cancro (AIRC);

Grant number: IG 2013 N. 14266 (MDR); **Grant sponsor:** Ente Cassa di Risparmio di Firenze and IstitutoToscanoTumori (LC);

Grant sponsor: post-doctoral fellowship of the Fondazione Italiana Per la Ricerca sul Cancro (FIRC) (Dr. Anastasia Chillà)

DOI: 10.1002/ijc.30817

History: Received 2 Feb 2017; Accepted 24 May 2017; Online 2 June 2017

Correspondence to: Lido Calorini, Department of Experimental and Clinical Biomedical Sciences, Section of Experimental Pathology and Oncology, University of Florence, Viale G.B. Morgagni, 50-Florence, 50134, Italy, E-mail: lido.calorini@unifi.it or Francesca Margheri, Department of Experimental and Clinical Biomedical Sciences, Section of Experimental Pathology and Oncology, University of Florence, Viale G.B. Morgagni, 50-Florence, 50134, Italy, E-mail: fmargheri@unifi.it

What's new?

Unlike normal cells, cancer cells use aerobic glycolysis to produce ATP. This study demonstrates the involvement of the uPA/uPAR system in the regulation of aerobic glycolysis. uPAR over-expression in human melanoma cells controls an invasive and a glycolytic phenotype in normoxic conditions. The uPAR activation-driven aerobic glycolysis depends on the $\alpha 5\beta 1$ -integrin-mediated uPAR connection with EGFR with engagement of the PI3K-mTOR-HIF α pathway. HIF-1 α trans-activates genes whose products mediate tumor invasion and glycolytic metabolism in melanoma cells, thus providing the common denominator between tumor metabolism and phenotypic invasive features. This study unveils the uPAR/IL-TKRs axis as a new pharmacological target for melanoma.

malignancy⁵ that may promote a metabolic reprogramming to oxidative phosphorylation, local invasion and metastatic dissemination, resistance to chemo and radiotherapy and suppression of anticancer immune responses [reviewed in Ref. 8]. In order to survive acidity cancer cells develop an acid-resistant phenotype, which is achieved by a HIF-1 α -dependent up-regulation of at least two important pH regulators, the monocarboxylate transporter-4 (MCT4)⁹ and the carbonic anhydrase-IX (CAIX).¹⁰

Data accumulated since the end of the 1990s put the members of the cell-associated fibrinolytic system (urokinase plasminogen activator and its receptor, uPA/uPAR) and plasminogen activator inhibitor type-1 (PAI1) at the first place of prognostic/predictive biomarkers of malignancy.^{11,12} Under HIF-1 α activity, hypoxia increases invasion of tumor cells by activating uPAR expression and signaling.^{13–17} Therefore, anaerobic glycolysis and uPAR overexpression in cancer cells are under the control of the common transcription factor HIF-1 α . Such a relation is even more compelling when considering our previous demonstration that following uPA/uPAR interaction, SV40-transformed human embryonic lung fibroblasts undergo an increase of glucose uptake dependent on translocation of GLUT1 from microsomal to membrane compartment and on GLUT2 activation.¹⁸ A correlation between migration and metabolic switch was recently reported by Bettum *et al.*,¹⁹ showing that in poorly motile melanoma cells the enhanced migration, drives a metabolic change to glycolysis. Thus, we have investigated on the metabolic implications of uPA/uPAR interaction in human melanoma cells, providing evidence that uPAR drives a glycolytic and invasive phenotype in melanoma cells in a EGFR-dependent fashion. We suggest that uPA/uPAR system on melanoma cells might represent a molecular link between invasion and glycolytic metabolism, disclosing a new target to inhibit both invasion and survival.

Materials and Methods**Cell lines and culture conditions**

Primary Human Epidermal Melanocytes were purchased from GIBCO Life Technologies Corporation (CA) and were grown in Medium 254CF with calcium plus Human Melanocytes Growth Supplement, obtained from the same company. The human melanoma cell lines A375 (MITF wild type, BRAF V600E, NRAS

wild type) and Mewo (harboring wild type BRAF and wild type NRAS) were obtained from American Type Culture Collection (Manassas, VA) and were grown in Roswell Park Memorial Institute medium (RPMI, Euroclone, Milano, Italy) containing 2 mM glutamine, 100 UI/ml penicillin, 100 μ g/ml streptomycin and supplemented with 10% FBS (Euroclone, Milano, Italy). A375-M6 melanoma cells (M6) were isolated in our laboratory from lung metastasis of SCID bg/bg mice i.v. injected with A375 cells. uPAR-negative human embryonic kidney-293 (HEK-293) cells transfected with cDNA of intact uPAR (uPAR-D1D2D3), with cDNAs corresponding to the truncated form of uPAR (uPAR-D2D3) and with pcDNA3 empty vector (no-uPAR), were kindly provided by Professor Pia Ragno (Napoli, Italy). HEK-293 transfected cells were maintained in DMEM containing 2 mM glutamine, 100 UI/ml penicillin, 100 μ g/ml streptomycin and supplemented with 10% fetal bovine serum (FBS; Euroclone). Mewo, A375, M6 and HEK-293 were independently validated by STR profiling by the DNA diagnostic centre BMR Genomics (Padova, Italy). Cells were amplified, stocked, and once thawed were kept in culture for a maximum of 4 months.

Antibodies and reagents

Antibodies and reagents are listed in Supporting Information 1: Supplementary Materials and Methods.

2-NBDG glucose uptake

The fluorescent-labeled glucose analog, 2-(N-(7-nitrobenz-2-oxa-1, 3-diazol-4-yl) amino-2-deoxyglucose (2-NBDG; Glucose Uptake Cell-Based Assay Kit, Cayman Chemical), was used to measure glucose uptake by cultured cells. Briefly, cells were washed 3 times for 1 min each, using ice-cold acid stripping buffer (100 mM NaCl, 50 mM glycine, pH 2.5) to remove any bound ligand from the receptors and then, were treated with different concentrations (1,8 nM for Mewo, 2,7 nM for A375, 3,6 nM for M6 and HEK-293) of exogenous uPA (human two-chain uPA isolated from human urine (CRINOS)) for 45 min in glucose-free culture medium containing 150 μ g/ml 2-NBDG. Apigenin, a flavonoid that has been reported to be an inhibitor of glucose transport, was used as negative control.²⁰ At the end of treatment, the cells were harvested, washed twice in Assay Buffer and analyzed by flow cytometer, measuring fluorescence in FL-1/FITC green channel (Emission 520 nm). For each measurement,

data from 10,000 single cell events were collected using a FACSCalibur (Beckman Coulter FC500) flow cytometer.

L-lactate measurement

Secreted L-lactate concentrations in cell-free culture supernatants were determined at room temperature using the Lactate Colorimetric Assay Kit (Bio Vision, Milpitas, CA), as to per manufacturer's instructions.

Western blotting and co-immunoprecipitation

Western blotting analyses were conducted as described previously.²¹ Cells were lysed in RIPA buffer (50 mM Tris-HCl, pH 8.0, 150 mM NaCl, 1% Nonidet P-40 (NP-40) or 0.1% Triton X-100) and 40 µg of total proteins were loaded on precast SDS-PAGE gels (Bio-Rad). Co-immunoprecipitation is described in Supporting Information 1: Supplementary Materials and Methods.

Immunofluorescence confocal microscopy

Immunofluorescence confocal microscopy and calculation of Mander coefficient for co-localization were performed as described.^{21,22}

RNA isolation and microarray analysis

Microarray data processing and statistical analysis are detailed in Supporting Information 1: Supplementary Materials and Methods. All microarray data have been deposited in the Gene Expression Omnibus (GEO) under the accession number GSE86383.

Quantitative real-time PCR analysis

Quantitative Real-Time PCR and the primers' sequences are reported in Supporting Information 1: Supplementary Materials and Methods.

siRNA for uPAR and EGFR knock-down

Targeting and not-targeting siRNAs were obtained from Dharmacon (Carlo Erba Reagents, Milan, Italy). Specific silencing of uPAR and EGFR genes was performed by transfection of M6 with small-interfering-RNA (siGENOMES-MARTpool), according to the manufactures' instructions. Not-targeting and GAPDH siRNA pool constructs were used as negative (siCONTROL) and positive control (siGAPD) respectively. To favor cell internalization siRNAs were incorporated into cationic liposomes, utilizing DharmaFECT transfection reagent. Cells were incubated with transfection mix (24–48 hr for mRNA analysis and 48 hr for protein and phenotypic analysis, respectively).

Xenograft model of human melanoma cancer and treatment with uPAR antisense oligo-deoxy-nucleotides (aODN) and antagonist peptides

Preparation of targeting uPAR aODN, non-targeting degenerated ODN (dODN) and of M25 peptide that inhibits uPAR-integrin interactions (targeting and not targeting) is detailed

in Supporting Information: Supplementary Materials and Methods.

All *in vivo* procedures were approved by the ethical committee of Animal Welfare Office of Italian Work Ministry and conformed to the legal mandates and Italian guidelines for the care and maintenance of laboratory animals. Twelve 8-week-old female athymic nude mice were purchased from Charles River. 1.5×10^6 M6 cells were injected in both flanks of nude mice. Animals were subdivided in 6 groups until tumors reached approximately 100 mm³. The animals were treated daily for three days: besides 2 untreated mice, treatments consisted in s.c. peri-tumoral administration of liposome-encapsulated vehicle alone (DOTAP), DOTAP + scramble ODN, DOTAP + uPAR-aODN, scramble M25 peptide (scM25) and M25 peptide. Upon sacrifice, isolated tumors were subjected to IHC for pyruvate-kinase M2 (PKM2). The immunohistochemical immunoperoxidase staining in tissue was quantified using Image J software, inverting the image to clean out the white noise, subtracting of the background and measuring the "integrated density".

Statistical analysis

Unless otherwise stated, all the experiments were performed five times in duplicate for a reliable application of statistics. Statistical analysis was performed with GraphPad Prism5 software. Values are presented as mean \pm SD. ANOVA and paired Student's *t* test were used to evaluate the statistical significance of differences between groups. The significance level was set at $p \leq 0.05$.

Results and Discussion

Melanoma cells are highly glycolytic and express a highly invasive phenotype

We used the Biological Process Ontology, to focus on differences among M6 melanoma cells and normal melanocytes (HeMa) in terms of glucose metabolism- and invasion-related transcripts obtained by microarray analysis. Table 1 shows that the most important up-regulations included glucose transporter-1 (GLUT-1); phosphoglucosmutase-2 (PGM2, which catalyzes the conversion of glucose 1-phosphate to glucose 6-phosphate, the starter of glycolysis); aldolase-A (ALDOA), that promotes the conversion of fructose 1,6-bisphosphate into glyceraldehyde 3-phosphate and dihydroxyacetone phosphate); enolase-1 (ENO-1, responsible for the conversion of 2-phosphoglycerate [PEG] to phosphoenolpyruvate [PEP]). It is worth to note that ENO-1 is a C-terminal lysine-containing plasminogen receptor accounting for enhanced plasmin-dependent invasiveness of uPAR co-expressing cells.²³ Melanoma cells showed high levels of pyruvate kinase-muscle type (PKM), which catalyzes the conversion of PEP to pyruvate, and thus ATP generation through activation of oxidative phosphorylation. Overexpression of pyruvate dehydrogenase kinase-1 (PDK1) drives the cells to the glycolytic pathway. Lactate dehydrogenase (LDH), which is also overexpressed in melanoma cells, catalyzes the

Table 1. Selected differentially expressed genes in A375 and M6 versus Hema.

Gene symbol	Gene name	Molecular process	Fold change (vs Hema)	
			A375	M6
GLUT1	Solute carrier family 2 (facilitated glucose transporter), member 1	Glucose transport	4,11	29,564
PGM2	Phosphoglucomutase 2	Glycolysis	20,886	46,843
PGM5	Phosphoglucomutase 5	Glycolysis		3,815
ALDOA	Aldolase A	Glycolysis	13,539	9,449
GAPDH	Glyceraldehyde-3-phosphate dehydrogenase	Glycolysis	3,031	2,869
ENO1	Enolase 1, (alpha)	Glycolysis	30,99	39,48
PKM	Pyruvate kinase, muscle	Glycolysis	10,396	5,12
PDK1	Pyruvate dehydrogenase kinase, isozyme 1	Reduced oxphos	5,448	6,208
LDH	Lactate dehydrogenase C	Lactate production	3,904	2,872
MCT4	Solute carrier family 16 (monocarboxylate transporter), member 1	Lactate/proton extrusion	2,719	2,571
BSG	Basigin, emprin	Lactate/proton extrusion	7,256	8,882
G6PD	Glucose-6-phosphate dehydrogenase	Pentose phosphate pathway	6,188	5,285
PLAUR	Plasminogen activator, urokinase receptor	Signal transduction	9,394	11,224
EGFR	Epidermal growth factor receptor	Signal transduction	27,168	28,304
AKT1S1	AKT1 substrate 1 (proline-rich)	Signal transduction	5,998	4,464
AKT2	v-akt murine thymoma viral oncogene homolog 2	Signal transduction	3,805	4,68
HIF1A	Hypoxia inducible factor 1, alpha subunit	Transcription factor	6,116	8,466
MMP2	Matrix metalloproteinase 2 (gelatinase A, 72kda gelatinase, 72kda type IV collagenase)	Cell invasion	5,535	2,208
MMP3	Matrix metalloproteinase 3 (stromelysin 1, progelatinase)	Cell invasion	–	2,736
MMP9	Matrix metalloproteinase 9 (gelatinase B, 92kda gelatinase, 92kda type IV collagenase)	Cell invasion	36,668	–
MMP14	Matrix metalloproteinase 14 (membrane-inserted)	Cell invasion	–3,726	–4,526
MMP16	Matrix metalloproteinase 16 (membrane-inserted)	Cell invasion	27,5	–
MMP17	Matrix metalloproteinase 17 (membrane-inserted)	Cell invasion	–5,084	–6.183
MMP19	Matrix metalloproteinase 19	Cell invasion	4,631	4,3578

conversion of pyruvate to lactate when oxygen is absent or in short supply. Upregulation of the monocarboxylate transporter MCT4, which is involved in the extrusion of lactate and its subunit basigin (BSG, CD147), also referred to as EMMPRIN (Extracellular Matrix Metalloproteinase inducer, so called after its metalloproteinase-inducing property)²⁴ accounts for tumor microenvironment acidification and for expression of a more invasive phenotype. Upregulation of glucose-6-phosphate dehydrogenase (G6PD), drives glucose metabolism to the pentose phosphate pathway (PPP), a major source of NADPH, required also for helping glycolytic cancer cells to meet their anabolic demands. The serine/threonine kinase Akt, the main inducer of the glucose-lactate pathway, was over-expressed in melanoma cells. Alongside, transcripts of recognized markers of malignancy, such as the alpha subunit of Hypoxia-Inducible Factor-1-alpha subunit (HIF-1 α), urokinase Plasminogen Activator Receptor (uPAR), and

Epidermal Growth Factor Receptor (EGFR) were strongly up-regulated. Overall, melanoma cells used in our study exhibit typical transcriptional features of a glycolytic phenotype, matched with high invasive markers (including increased expression of several matrix metallo-proteinases, table1). Indeed, metastasis-prone M6 cells stopped growing in a glucose-free medium, thus disclosing a glucose-addicted metabolism (Fig. 1a). In agreement with the HIF-1 α -dependent stimulation of the glycolytic pathway, HIF-1 α was over-expressed in melanoma cells, a feature that accounts for the simultaneous expression of a glycolytic and invasive phenotype.²⁵ It is not surprising that a factor induced by hypoxia could regulate cellular metabolism even under conditions of normal oxygen tension, such as those of our experiments. Actually, in cancer cells HIF-1 α can undergo an oncogenic activation²⁶ also under normoxic conditions^{6,27} indicating that activation of the glycolytic pathway in cancer is an effect

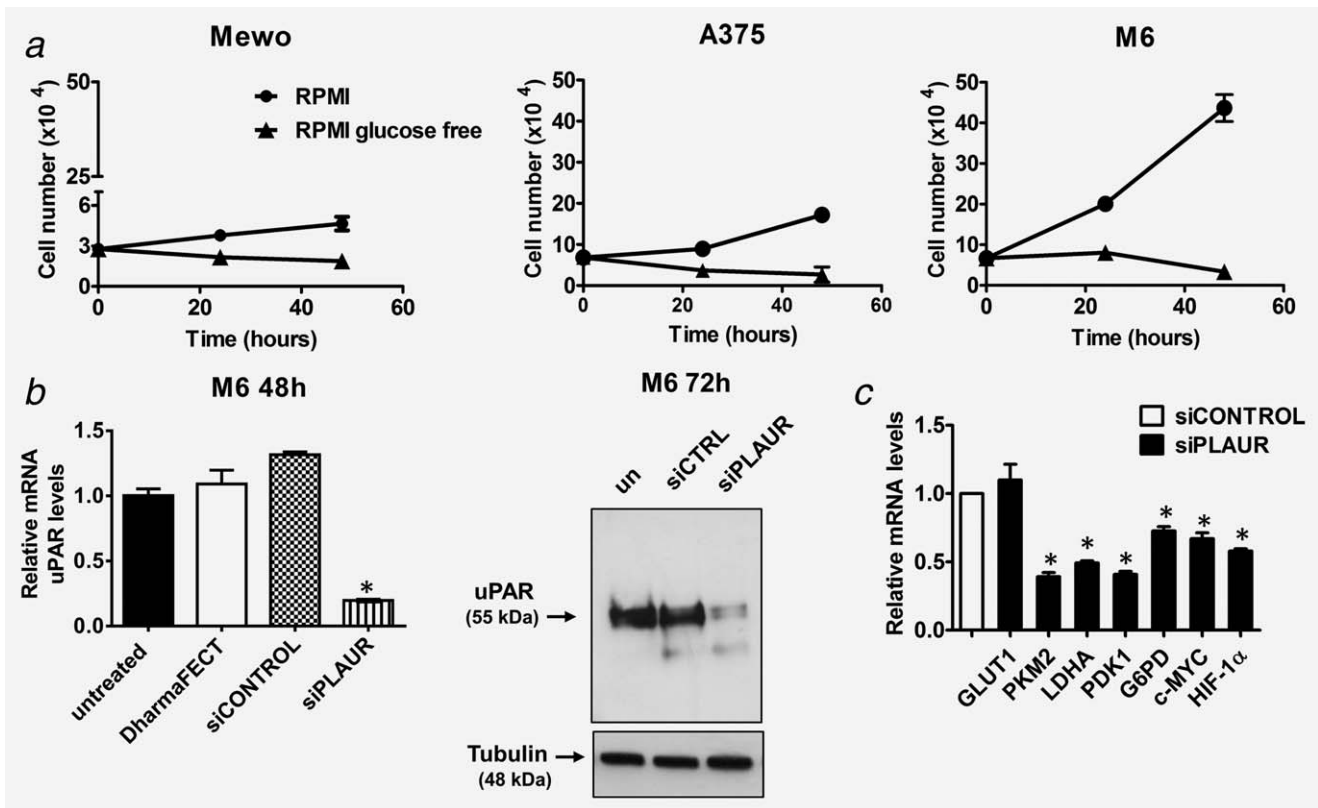


Figure 1. Glucose-dependence of malignant melanoma cells growth, and downregulation of glycolytic enzymes following uPAR silencing in A375-M6 (M6) melanoma cells. (a) growth of Mewo, A375 and M6 melanoma cells after glucose deprivation is a function of malignancy. (b) induction of uPAR downregulation by specific siRNA treatment in M6 cells; DharmaFECT: cells treated with vehicle alone; siCONTROL: not targeting siRNA; siPLAUR: anti uPAR siRNA. (c) relative expression of glycolytic enzymes and of glycolysis-related transcription factors after uPAR downregulation with siRNAs, taking the value of each control as 1.0. Error bars: mean \pm SD; * $P < 0.05$.

of genome instability leading to reprogramming pyruvate oxidation to lactic acid conversion. Moreover, HIF-1 α also controls expression of MMP9 and of uPAR.^{15,28}

uPAR downregulation and uPA stimulation, both suggest an uPAR-dependent glycolytic phenotype in A375-M6 melanoma cells

With respect to normal melanocytes and MeWo, the uPAR molecule is strongly up-regulated in A375 and M6 melanoma cells.²⁹ uPAR silencing by specific siRNA smart pools (siPLAUR) was used to investigate uPAR-dependent expression of glycolysis enzymes. After validating the silencing activity of siPLAUR (Fig. 1b), we have studied uPAR-dependent expression of several glycolytic enzymes over-expressed in these melanoma cells (Fig. 1c). We found that expression of LDHA, PDK1, G6PDH was significantly down-regulated by uPAR silencing. Since the microarray analysis did not discriminate between PKM1 (an isoform expressed in normal tissues of adults) and PKM2, the embryonic isoform exclusively expressed in tumors, we focused our attention on the latter, which has been proved to be critical for driving tumor metabolism to the Warburg effect³⁰: uPAR silencing produced a down-regulation of PKM2. Although uPAR silencing did not modify GLUT1 expression (Fig. 1c), the binding of uPA to uPAR, after 45 min

exposure to uPA, produced an enrichment of GLUT1 at the cell membrane (Figs. 2a and 2b). Immunofluorescence with anti-GLUT1 antibodies showed that under resting conditions GLUT1 has a prevalent peri-nuclear and membrane location, which shifts to a prevalent membrane granular location upon uPAR activation (Fig. 2c), accounting for an increase of glucose uptake. Indeed, FACS analysis used to study both uPAR silencing and 2-NBDG uptake, revealed that uPAR downregulation induced a decrease of NBDG uptake (Fig. 2d). To show a direct correlation between glucose uptake and uPAR expression, we have compared 2-NBDG uptake in MeWo and in M6 which express higher amounts of uPAR than MeWo.²⁹ 2-NBDG uptake was measured under basal conditions and upon uPAR activation following uPA addition, in the absence and in the presence of apigenin, a specific glucose uptake inhibitor. In M6 glucose uptake was higher than in MeWo, either under basal conditions or on uPAR activation, which amplifies the difference of 2-NBDG uptake between the two melanoma cell lines (Fig. 2e). Furthermore, binding of uPA to uPAR increases PKM2 protein levels, without affecting PKM1 (Fig. 1f). Again, stimulation with uPA in siPLAUR M6 melanoma cells did not cause any change in PKM2 expression, proving that this effect is dependent by uPA/uPAR interaction (Fig. 1f). To avoid intracellular acidosis, glycolytic melanoma cells need to extrude

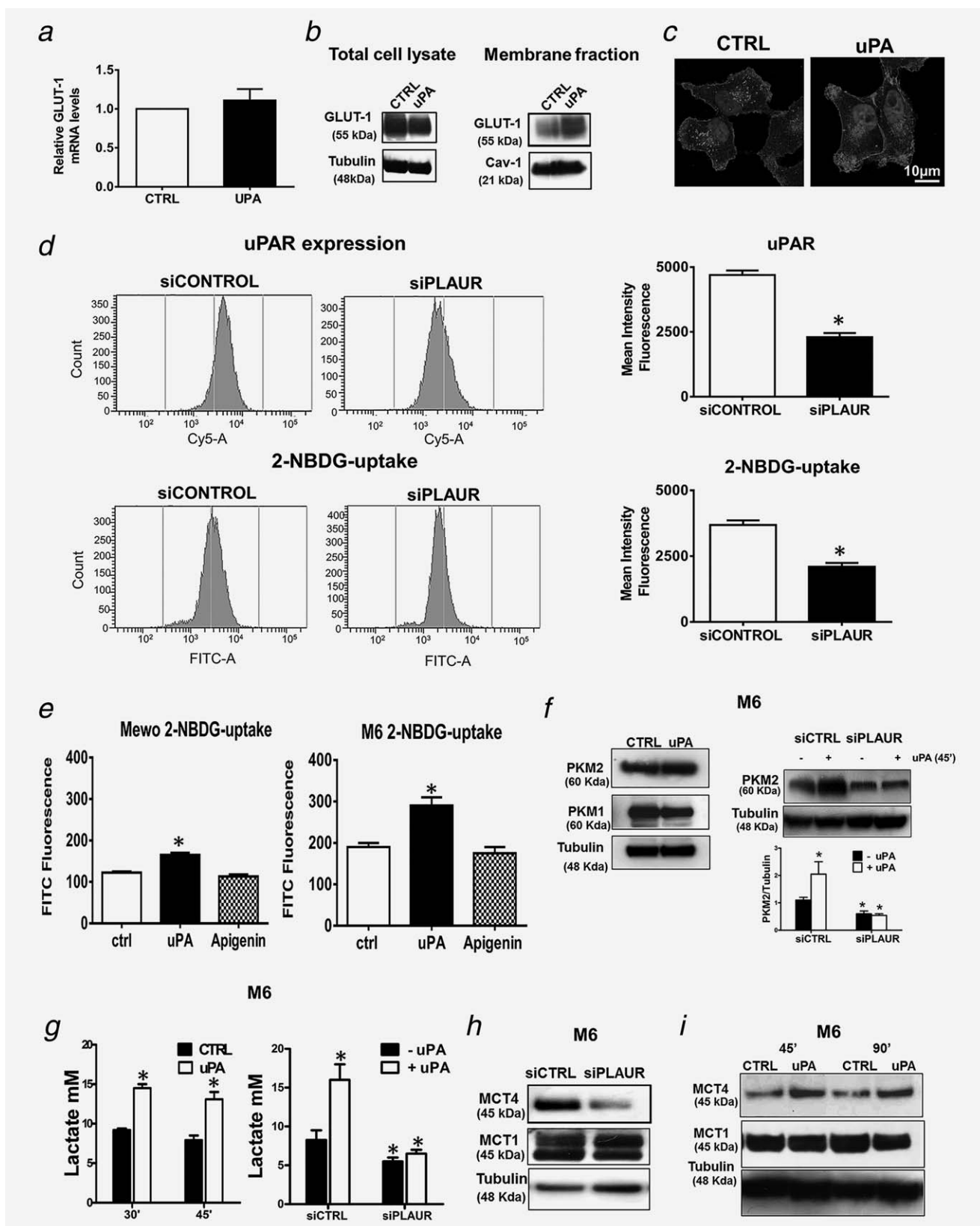


Figure 2. Regulation of glucose uptake/metabolism and of lactate extrusion by the uPA/uPAR system. (a) expression level of GLUT-1 transcription M6 cells after uPA 3,6 nM stimulation. (b) GLUT-1 protein in the total cell lysate and in the membrane fraction following uPA 3,6 nM stimulation. (c) immunofluorescence of GLUT-1 in M6 after uPA 3,6 nM stimulation, showing GLUT-1 enrichment at the cell membrane after 45 min. (d) flow cytometry of uPAR expression after uPAR silencing by uPAR siRNA (upper lane) and uptake of 2-NBDG (lower lane) in M6 cells. Histograms on the right show quantification. (e) Quantification of the fluorescence probe (2-NBDG) uptake in Mewo melanoma cells (upper lane) and in M6 melanoma cells (lower lane) following 45 min stimulation with uPA 1,8 nM and 3,6 nM respectively. (f) Western blotting of PKM1 and PKM2 isoforms in M6 after uPA 3,6 nM stimulation for 45 min (upper panel) and western blotting of PKM2 in siCTRL and siPLAUR M6 after uPA stimulation for 45 min (lower panel). Histogram below show PKM2 normalization. (g) lactate production in M6 after 30 min and 45 min uPA stimulation (3,6 nM) (on the left) and in siCTRL and siPLAUR cells after 45 min uPA stimulation (3,6 nM) (on the right). (h) Western blotting of monocarboxylate transporters MCT1 and MCT4 in M6. (i) time-dependent uPA 3,6 nM stimulation of MCT1 and MCT4 in M6. Each panel of this figure shows a typical experiment out of five experiments that gave similar results. Error bars: mean \pm SD; * $P < 0.05$.

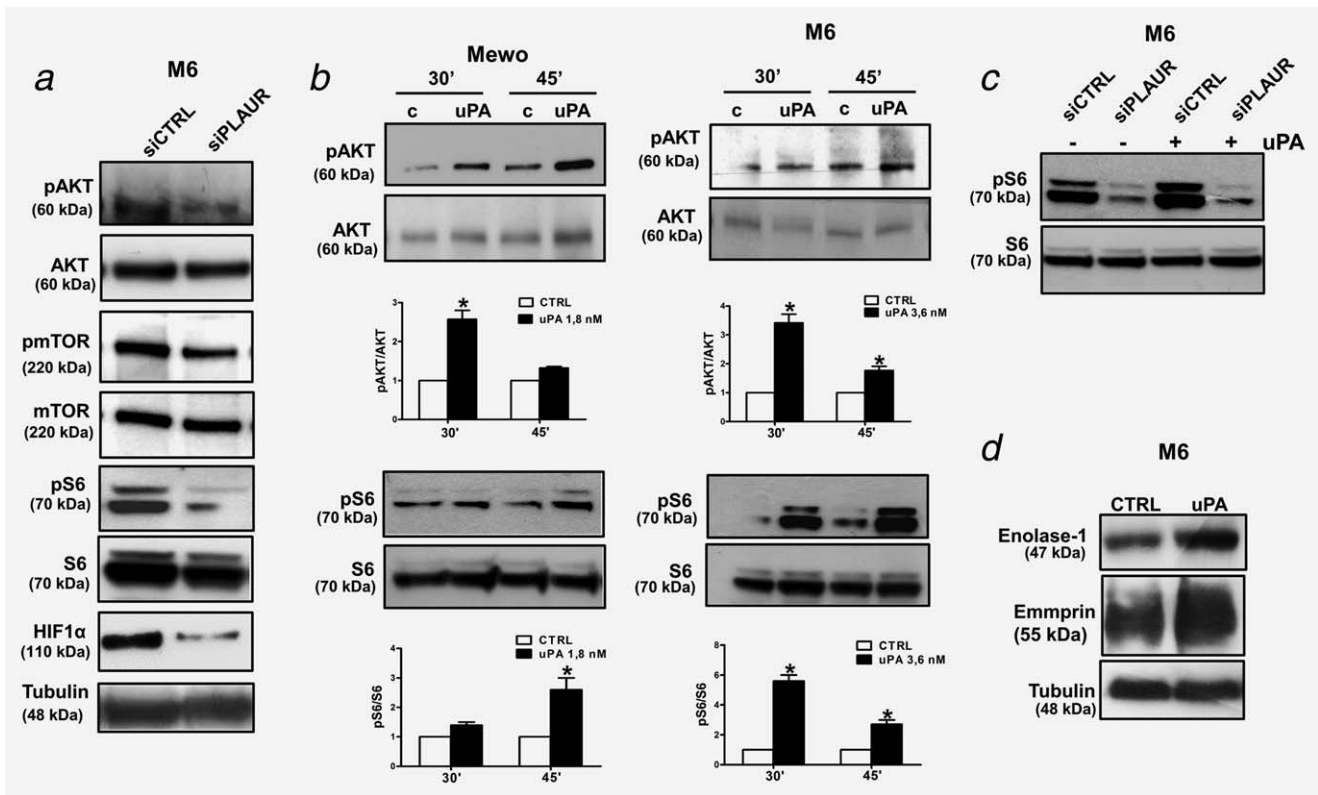


Figure 3. Metabolic transducers of uPA/uPAR system in melanoma cells, and uPA-dependent up-regulation of pro-invasive regulatory molecules. (a) down-regulation of the pAKT/pmTOR/pS6K/HIF-1 α axis following siRNA-dependent uPAR silencing. (b) uPA-dependent stimulation of AKT and pS6K phosphorylation in Mewo (1,8 nM) and M6 cells (3,6 nM). Histograms show the quantification (c) uPA-dependent stimulation (3,6 nM for 45') of S6 in siCTRL and siPLAUR cells. (d) uPA-dependent up-regulation of enolase-1 and EMMPRIN in M6. Each panel shows a typical experiment out of five experiments that gave similar results. Error bars in the histograms of uPA stimulation: mean \pm SD; * $P < 0.05$.

lactate through MCT4, whose expression is higher in melanoma cells than in normal melanocytes (table 1). We measured lactate production in M6 cells and observed that uPAR activation with uPA augmented lactate production (Fig. 2g, histogram on the left) while the stimulation with uPA in siPLAUR cells did not produce any increment in lactate extrusion, as compared to siCTRL cells (Fig. 2g, histogram on the right). Further, we found that MCT4 is under the control of uPAR, as proven by its decrease upon uPAR silencing, while the amount of MCT1, which entails lactate uptake, was uPAR-independent. (Fig. 2h). The effects on MCT4 were amplified upon uPA stimulation (Fig. 2i). On the whole, these data show that uPAR is critical in participating to sustain a glycolytic trait in melanoma cells.

uPAR silencing, uPA stimulation and metabolic transducers in melanoma cells

As previously demonstrated, uPAR promotes cancer cell growth through the PI3K/AKT pathway.³¹ In M6 melanoma cells treated with siPLAUR, we found a strong reduction of PI3K/AKT/mTOR signaling (Fig. 3a). Further, we demonstrated that pAKT and pS6 are controlled by binding of uPA to uPAR in a time-dependent fashion in both Mewo and M6 melanoma cells (Fig. 3b). We observed also that uPA stimulation (3,6 nM for 45') does not result into S6

hyper-phosphorylation in siPLAUR, with respect to siCTRL, proving that S6 activation is mediated by uPA/uPAR interaction (Fig. 3c). One of the primary functions of activated AKT is to phosphorylate the mammalian target of rapamycin (mTOR), a regulator of cell proliferation, cellular energy status, and oxygen level. In cancer cells, mTOR induces S6 p70 kinase and HIF1 α ^{6,7} whose activation, as well as the activation of the whole PI3K/AKT axis, is regulated also by uPAR. In turn, mTOR directly stimulates mRNA translation and ribosome biogenesis and activates HIF-1 α , even under normoxic conditions.^{6,27} Therefore, HIF-1 α expression may be one the terminal links of the uPAR-triggered chain, as suggested by HIF-1 α reduction consequent to uPAR downregulation in M6 cells (Figs. 1c and 3a). Figure 1c also shows the control exerted by uPAR modulation on cMYC expression, the second important terminal component of the PI3K/AKT signaling pathway.³² This data is in agreement with the observation that MYC activation can collaborate with HIF-1 α to confer metabolic advantages to tumor cells.³³

Further, we have shown that uPAR activation by uPA also up-regulates expression of enolase-1 and EMMPRIN, molecules that bridge glycolysis and lactate homeostasis with the invasive properties of cancer cells^{23,24} (Fig. 3d).

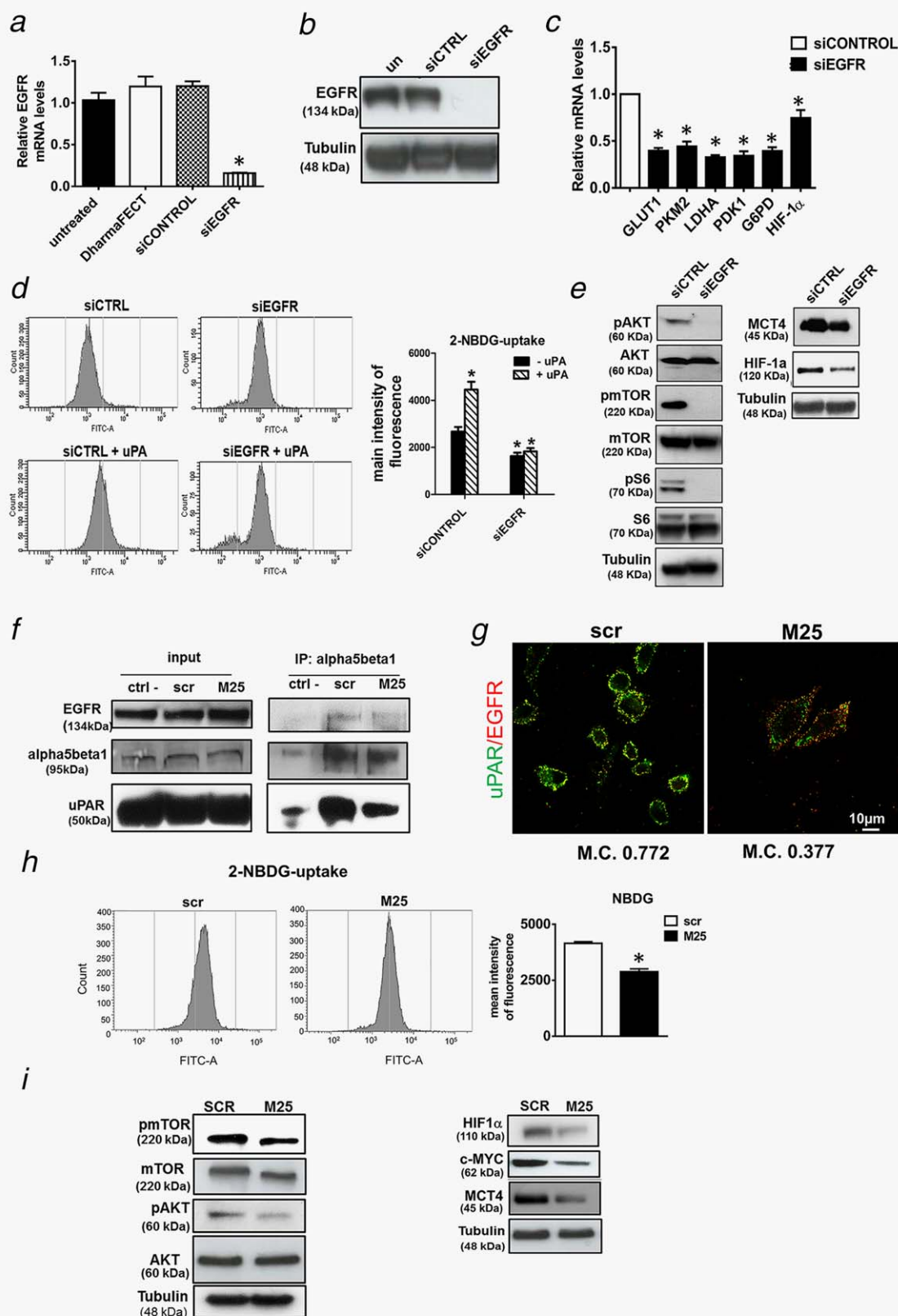


Figure 4. EGFR silencing and its uncoupling from uPAR by IL-TKR/uPAR antagonist M25 strongly impacts on glucose metabolism and signaling pathways in A375-M6 cells. (a, b) effect of siRNA for EGFR (siEGFR) at RNA and protein levels, respectively (un, untreated; siCTRL, not targeting siRNA). (c) relative gene expression of glycolysis transcript after EGFR silencing. (d) 2-NBDG uptake in siCTRL and siEGFR M6 cells after uPA 3, 6 nM stimulation for 45 min. Histogram on the right show quantification. (e) western blotting of pAKT, pmTOR, pS6K, HIF1a, and MCT4 after siRNA-dependent EGFR silencing. (f) co-immunoprecipitation of EGFR and uPAR by the integrin antagonist M25 (refer to Supplementary M&M); (g) confocal microscopy of uPAR (green) and EGFR (red) under the effect of the scramble (scr) and M25 peptide: M.C. = Mander coefficient indicating full co-localization (value of 1.0) or partial co-localization (values lower than 1.0) (24, 25). (h) flow cytometry of 2-NBDG uptake under control conditions (scr) and under M25 peptide; the histogram on the right show quantification. (i) Western blots of pAKT, pmTOR, HIF1a, c-MYC and MCT4 under the effect of the scramble (scr) and M25 peptide. Each panel shows a typical experiment out of five experiments that gave similar results. Error bars: mean \pm SD; * $p < 0.05$.

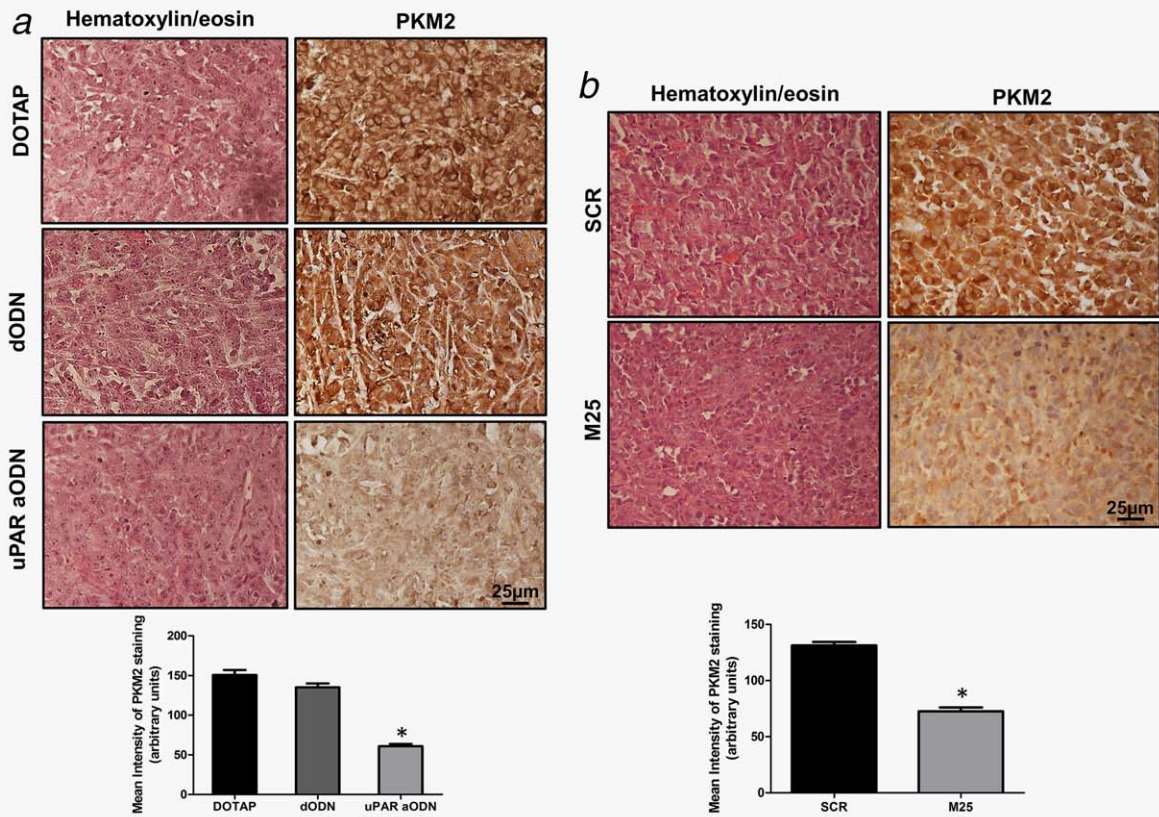


Figure 5. uPAR silencing and its uncoupling from IL-TKRs strongly reduces PKM2 in xenografted human melanoma. (a) IHC of PKM2 after treatment with the vector alone (DOTAP), degenerated ODNs (dODN) and uPAR-aODNs (aODN). Histograms show the quantification of PKM2 staining (b) IHC of PKM2 after treatment with a scramble peptide (SCR) and with peptide M25 which uncouples uPAR/integrin/IL-TKRs interactions. 25 μ M, scale bar. Figures are representative of results obtained from four explanted tumors for each condition. Histograms report the quantification of PKM2 staining. Error bars: mean \pm SD; * $p < 0.05$.

Native uPAR is organized in three differently folded domains (D1, D2 and D3 from the N terminus), stabilized by disulfide bonds, and uPA directly interacts with D1 in a pocket formed by all three domains.³⁴ uPAR may be anchored to the cell surface either in its native form (D1D2D3) or in a truncated form (D2D3), as a result of a cleavage of D1-D2 linker region.³⁵ Further, removal of D1 abolishes the lateral interaction of uPAR with integrins and its capability to regulate integrin functions.³⁶ Therefore, by using the uPAR-negative human embryonic kidney-293 (HEK-293) cells transfected with cDNA of intact uPAR (uPAR-D1D2D3), with cDNAs corresponding to the truncated form of uPAR (uPAR-D2D3) and with pcDNA3 empty vector (no-uPAR)³⁶ we evaluated what form of uPAR was involved in GLUT activation and glucose uptake (Supporting Information Fig. 1). We have shown that glucose uptake is dependent on the D1D2D3 form. However, uPAR D2D3 cells are sensitive to glucose deprivation, although less than uPAR D1D2D3, probably because the truncated form of uPAR, which retains sequence-specific integrin binding sites, is able to partially induce integrins and EGFR activation.

uPAR-coupled EGFR mediates the glycolytic phenotype in melanoma cells

uPAR is anchored to the cell membrane by glycosylphosphatidylinositol (GPI), a feature requiring signalling partners. Already established uPAR-mediated pathways include an integrin-dependent uPAR association with the four IL-TKR systems EGFR, IGFR, PDGFR and MET.³⁷ Such IL-TKRs also regulate glucose uptake and glycolysis in many cell types and in cancer cells.^{38–41} Dependent on the cell type, different integrins mediate uPAR interaction with partner molecules. Mechanistic analysis implicated high uPAR expression, its interaction with and activation of $\alpha 5\beta 1$ -integrin and activation of EGFR signaling, as determinants of the *in vivo* growth promotion in several cell lines, including melanoma.^{37,42, 43} Such considerations, coupled with the already reported impact of EGFR signaling on glucose metabolism³⁸ prompted us to verify whether the uPAR-driven glycolytic phenotype of melanoma cells is sustained by an integrin-mediated uPAR/EGFR interplay. We demonstrated that EGFR silencing (Figs. 4a and 4b) induces down-regulation of several glycolytic enzymes in melanoma cells (Fig. 4c), in parallel with down-regulation of HIF1 α (Figs. 4c and 4e) and a decrease of

NBDG uptake (Fig. 4d). uPA stimulation in siEGFR M6 cells did not affect glucose-uptake, demonstrating that the uPAR-mediated glycolytic phenotype is dependent on EGFR activation (Fig. 4d). Again EGFR silencing induces a strong reduction of PI3K/AKT/mTOR signaling (Fig. 4e), similarly to that observed after uPAR downregulation. As we have previously shown that M6 melanoma cells express a relevant amount of $\alpha 5\beta 1$ integrin,²² the main partner that interconnects uPAR with EGFR⁴² we reasoned that the property of M25 peptide to uncouple uPAR from integrins, and hence from its partner IL-TKR (including EGFR) could mime uPAR silencing on melanoma cell signaling. Immunoprecipitation of M6 lysates demonstrated the activity of M25 in uncoupling uPAR- $\alpha 5\beta 1$ interaction (Fig. 1f), as confirmed by confocal microscopy (Fig. 4g). Treatment of cells with 50 μ M M25 for 30' at 37°C induced a significant decrease of 2-NBDG uptake (Fig. 4h), a down-regulation of phosphorylation of mTOR and AKT and a loss of HIF1 α , cMYC and MCT4 (Fig. 4i). Therefore, first we have shown that EGFR and uPAR interaction is down-regulated by a peptide that competes for uPAR/ $\alpha 5\beta 1$ binding. Second, EGFR and uPAR silencing result into down-regulation of 2-NBDG uptake, of the same glycolytic transcripts and of HIF-1 α . Third, uPAR-driven glycolytic functions decrease in the presence of the integrin antagonist peptide. Moreover, the master glycolysis signaling pathway PI3K/pAKT/mTOR/HIF-1 α , that is upregulated following uPAR activation, also commands EGFR-dependent glycolysis.⁴⁴

Xenograft model of human melanoma cancer in athymic nude mice and treatment with uPAR antagonists

To validate our observations *in vivo*, we analyzed samples obtained by M6 melanoma cells xenografts treated daily for

three days with s.c. peri-tumoral injections of liposomes-encapsulated uPAR-aODN/dODN or with M25/sM25 peptides, once tumors reached approximately 100 mm³. ODNs were encapsulated in liposomes to favor their cellular uptake, while the peptides were injected as such considering their activity on cell surface uPAR, IL-TKR and integrins. Four days after the beginning of treatment, animals were sacrificed. PKM2 was used as a glycolytic marker of melanoma xenografts. No significant differences in tumor size were observed between untreated tumors and tumors treated daily for three days with uPAR-aODN/dODN or with M25/sM25 peptides. IHC performed on tumor slices at the end of treatment showed that both uPAR downregulation and uPAR/IL-TKR uncoupling by M25 peptide produced a loss of PKM2, as compared with untreated tumors and tumors treated with vehicles or irrelevant molecules (Fig. 5).

Conclusions

uPAR over-expression in human melanoma cells controls an invasive and a glycolytic phenotype in normoxic conditions. The uPAR activation-driven Warburg effect depends on the $\alpha 5\beta 1$ -integrin-mediated uPAR connection with EGFR in melanoma cells with engagement of the PI3K-mTOR-HIF α pathway. HIF-1 α trans-activates genes whose products mediate tumor invasion and glycolytic metabolism in melanoma cells, thus providing the common denominator between tumor metabolism and the phenotypic invasive features.

Acknowledgements

No potential conflicts of interest were disclosed.

REFERENCES

- Vander Heiden MG, Cantley LC, Thompson CB. Understanding the Warburg effect: the metabolic requirements of cell proliferation. *Science* 2009; 324:1029–33
- Jadvar H, Alavi A, Gambhir SS. 18F-FDG uptake in lung, breast, and colon cancers: molecular biology correlates and disease characterization. *J Nucl Med* 2009; 50:1820–7.
- Gillies RJ, Gatenby RA. Adaptive landscapes and emergent phenotypes: why do cancers have high glycolysis? *J Bioenerg Biomembr* 2007; 39:251–7.
- Smallbone K, Gatenby RA, Gillies RJ, Maini PK, Gavaghan DJ. Metabolic changes during carcinogenesis: potential impact on invasiveness. *J Theor Biol* 2007; 244:703–13.
- Pinheiro C, Longatto-Filho A, Azevedo-Silva J, Casal M, Schmitt FC, Baltazar F. Role of monocarboxylate transporters in human cancers: state of the art. *J Bioenerg Biomembr* 2012; 44:127–39.
- Cairns RA, Harris IS, Mak TW. Regulation of cancer cell metabolism. *Nat Rev Cancer* 2011; 11: 85–95.
- Peppicelli S, Bianchini F, Calorini L. Extracellular acidity, a “reappreciated” trait of tumor environment driving malignancy: perspectives in diagnosis and therapy. *Cancer Metastasis Rev* 2014; 33:823–32.
- Parks SK, Chiche J, Pouyssegur J. Disrupting proton dynamics and energy metabolism for cancer therapy. *Nat Rev Cancer* 2013; 13:611–23.
- Ullah MS, Davies AJ, Halestrap AP. The plasma membrane lactate transporter MCT4, but not MCT1, is up-regulated by hypoxia through a HIF-1 α -dependent mechanism. *J Biol Chem* 2006; 281:9030–7.
- Chiche J, Ilc K, Laferrière J, Trottier E, Dayan F, Mazure NM, Brahimi-Horn MC, Pouyssegur J. Hypoxia-inducible carbonic anhydrase IX and XII promote tumor cell growth by counteracting acidosis through the regulation of the intracellular pH. *Cancer Res* 2009; 69:358–68.
- Schmitt M, Mengele K, Napieralski R, Magdolen V, Reuning U, Gkazepis A, Sweep F, Brünner N, Foekens J, Harbeck N. Clinical utility of level-of-evidence-1 disease forecast cancer biomarkers uPA and its inhibitor PAI-1. *Expert Rev Mol Diagn* 2010; 10:1051–67.
- Mengele K, Napieralski R, Magdolen V, Reuning U, Gkazepis A, Sweep F, Brünner N, Foekens J, Harbeck N, Schmitt M. Characteristics of the level-of-evidence-1 disease forecast cancer biomarkers uPA and its inhibitor PAI-1. *Expert Rev Mol Diagn* 2010; 10:947–62.
- Graham CH, Fitzpatrick TE, McCrae KR. Hypoxia stimulates urokinase receptor expression through a heme protein-dependent pathway. *Blood* 1998; 91:3300–7.
- Graham CH, Forsdike J, Fitzgerald CJ, Macdonald-Goodfellow S. Hypoxia-mediated stimulation of carcinoma cell invasiveness via upregulation of urokinase receptor expression. *Int J Cancer* 1999; 80:617–23.
- Krishnamachary B, Berg-Dixon S, Kelly B, Agani F, Feldser D, Ferreira G, Iyer N, LaRusch J, Pak B, Taghavi P, Semenza GL. Regulation of colon carcinoma cell invasion by hypoxia-inducible factor 1. *Cancer Res* 2003; 63:1138–43.
- Rofstad EK, Rasmussen H, Galappathi K, Mathiesen B, Nilsen K, Graff BA. Hypoxia promotes lymph node metastasis in human melanoma xenografts by up-regulating the urokinase-type plasminogen activator receptor. *Cancer Res* 2002; 62:1847–53.
- Rofstad EK, Mathiesen B, Galappathi K. Increased metastatic dissemination in human

- melanoma xenografts after sub-curative radiation treatment: radiation-induced increase in fraction of hypoxic cells and hypoxia-induced up-regulation of urokinase-type plasminogen activator receptor. *Cancer Res* 2004; 64:13–8.
18. Anichini E, Zamperini A, Chevanne M, Caldini R, Pucci M, Fibbi G, Del Rosso M. Interaction of urokinase-type plasminogen activator with its receptor rapidly induces activation of glucose transporters. *Biochemistry* 1997; 36:3076–83.
 19. Bettum IJ, Gorad SS, Barkovskaya A, Pettersen S, Moestue SA, Vasiliauskaitė K, Tenstad E, Øyjord T, Risa Ø, Nygaard V, Mælandsmo GM, Prasmickaite L. Metabolic reprogramming supports the invasive phenotype in malignant melanoma. *Cancer Lett* 2015; 366:71–83.
 20. Melstrom LG, Salabat MR, Ding XZ, Milam BM, Strouch M, Pelling JC, Bentrem DJ. Apigenin inhibits the GLUT-1 glucose transporter and the phosphoinositide 3-kinase/Akt pathway in human pancreatic cancer cells. *Pancreas* 2008; 37:426–31.
 21. Margheri F, Chillà A, Laurenzana A, et al. Endothelial progenitor cell-dependent angiogenesis requires localization of the full-length form of uPAR in caveolae. *Blood* 2011; 118:3743–55.
 22. Margheri F, Luciani C, Taddei ML, et al. The receptor for urokinase-plasminogen activator (uPAR) controls plasticity of cancer cell movement in mesenchymal and amoeboid migration style. *Oncotarget* 2014 Mar 30; 5:1538–53.
 23. Deryugina EI, Quigley JP. Cell surface remodeling by plasmin: a new function for an old enzyme. *J Biomed Biotechnol* 2012; 2012:564259.
 24. Yan L, Zucker S, Toole BP. Roles of the multifunctional glycoprotein, emmprin (basigin; CD147), in tumour progression. *Thromb Haemost* 2005; 93:199–204.
 25. Pouyssegur J, Dayan F, Mazure NM. Hypoxia signalling in cancer and approaches to enforce tumor regression. *Nature* 2006; 441:437–43.
 26. Denko NC. Hypoxia, HIF1 and glucose metabolism in the solid tumor. *Nat Rev Cancer* 2008; 8: 705–13.
 27. Majumder PK, Febbo PG, Bikoff R, et al. mTOR inhibition reverses Akt-dependent prostate intraepithelial neoplasia through regulation of apoptotic and HIF-1-dependent pathways. *Nat Med* 2004; 10:594–601.
 28. Semenza GL. Targeting HIF-1 for cancer therapy. *Nature Rev Cancer* 2003; 3:721–32.
 29. Laurenzana A, Biagioni A, Bianchini F, Peppicelli S, Chillà A, Margheri F, Luciani C, Pimpinelli N, Del Rosso M, Calorini L, Fibbi G. Inhibition of uPAR-TGF β crosstalk blocks MSC-dependent EMT in melanoma cells. *J Mo Med (Berl)* 2015; 93:783–94.
 30. Christofk HR, Vander Heiden MG, Harris MH, Ramanathan A, Gerszten RE, Wei R, Fleming MD, Schreiber SL, Cantley LC. The M2 splice isoform of pyruvate kinase is important for cancer metabolism and tumour growth. *Nature* 2008; 452:230–3.
 31. Nowicki TS, Zhao H, Darzynkiewicz Z, Moscatello A, Shin E, Schantz S, Tiwari RK, Geliebter J. Downregulation of uPAR inhibits migration, invasion, proliferation, FAK/PI3K/Akt signaling and induces senescence in papillary thyroid carcinoma cells. *Cell Cycle* 2011; 10:100–7.
 32. Hirschhaeuser F, Sattler UG, Mueller-Klieser W. Lactate: a metabolic key player in cancer. *Cancer Res* 2011; 71:6921–5.
 33. Dang CV, Kim JW, Gao P, Yuste J. The interplay between MYC and HIF in cancer. *Nat Rev Cancer* 2008; 8:51–6.
 34. Llinas P, Le Du MH, Gardsvoll H, Dano K, Ploug M, Gilquin B, Stura EA, Ménez A. Crystal structure of the human urokinase plasminogen activator receptor bound to an antagonist peptide. *Embo J* 2005; 24:1655–63.
 35. Ploug M. Identification of specific sites involved in ligand binding by photoaffinity labeling of the receptor for the urokinase-type plasminogen activator. Residues located at equivalent positions in uPAR domains I and III participate in the assembly of a composite ligand-binding site. *Biochemistry* 1998; 37:16494–505.
 36. Montuori N, Carriero MV, Salzano S, Rossi G, Ragno P. The cleavage of the urokinase receptor regulates its multiple functions. *J Biol Chem* 2002; 277:46932–9.
 37. Eden G, Archinti M, Furlan F, Murphy R, Degryse B. The urokinase receptor interactome. *Curr Pharm Des* 2011; 17:1874–1889.
 38. Kaplan O, Jaroszewski JW, Faustino PJ, Zugmaier G, Ennis BW, Lippman M, Cohen JS. Toxicity and effects of epidermal growth factor on glucose metabolism of MDA-468 human breast cancer cells. *J Biol Chem* 1990; 265:13641–9.
 39. Ran C, Liu H, Hitoshi Y, Israel MA. Proliferation-independent control of tumor glycolysis by PDGFR-mediated AKT activation. *Cancer Res* 2013; 73:1831–43.
 40. Shefi-Friedman L, Wertheimer E, Shen S, Bak A, Accili D, Sampson SR. Increased IGF1 activity and glucose transport in cultured skeletal muscle from insulin receptor null mice. *Am J Physiol Endocrinol Metab* 2001; 281:E16–24.
 41. Perdomo G, Martinez-Brocca MA, Bhatt BA, Brown NF, O'Doherty RM, Garcia OA. Hepatocyte growth factor is a novel stimulator of glucose uptake and metabolism in skeletal muscle cells. *J Biol Chem* 2008; 283:13700–6.
 42. Liu D, Aguirre Ghiso JA, Estrada Y, Ossowski L. EGFR is a transducer of the urokinase receptor initiated signal that is required for in vivo growth of a human carcinoma. *Cancer Cell* 2002; 1:445–457.
 43. Aguirre-Ghiso JA, Estrada Y, Liu D, Ossowski L. ERK(MAPK) activity as a determinant of tumor growth and dormancy; regulation by p38(SAPK). *Cancer Res* 2003; 63:1684–95.
 44. Simons AL, Orcutt KP, Madsen JM, Scarbrough PM, Spitz DR. The role of Akt pathway signaling in glucose metabolism and metabolic oxidative stress. In: Spitz DR, Dornfeld KJ, Krishnan K, Gius D, eds. *Oxidative stress in cancer biology and therapy*. New York: Springer Science & Business Media, 2012. 21–46.